Estimation of evapotranspiration using three-temperature model based on MODIS data

XIONG Yujiu[1, 2], QIU Guoyu[3], CHEN Xiaohong[1, 2], ZHAO Shaohua[4], TIAN Fei[5]

1. *Department of Water Resources and Environment*, *School of Geography and Planning*, *Sun Yat-sen University*, *Guangzhou* 510275, *China*;
2. *Key Laboratory of Water Cycle and Water Security in Southern China of Guangdong High Education Institute*, *Sun Yat-sen University*, *Guangzhou* 510275, *China*;
3. *School of Environment and Energy*, *Shenzhen Graduate School of Peking University*, *Shenzhen* 518055, *China*;
4. *Environmental Satellite Center*, *Ministry of Environmental Protection*, *Beijing* 100094, *China*;
5. *College of Resources Science and Technology*, *Beijing Normal University*, *Beijing* 100875, *China*

Abstract: Estimation of evapotranspiration (ET) is an obstacle in researches of both water and energy balance. In this paper, three-temperature (3T) model was revised for remote sensing application. A case study was performed in a semi-arid grassland from July to October in 2008 in Taibus Banner of Inner Mongolia, China. Eleven cloudless MODIS images at 1 km scale were used to estimate ET and data observed from two Bowen ratio systems in the corresponding period was adopted to validate the performance of the 3T model. Results showed that: (1) the modeled ET varied from 1.28 mm/d to 9.03 mm/d in the growing season, with a mean value of 4.58 mm/d; (2) the modeled daily ET distributed homogeneously in space, and temporally, ET value increased and then decreased gradually as the growing season changed from beginning to the end; (3) the mean absolute error between the observed and modeled ET was 0.58 mm/d, with maximum and minimum absolute errors of 1.64 mm/d and 0.11 mm/d, respectively, and the mean absolute percent error was 17.10%. All the performances indicated that the 3T model has a good potential in ET estimation.

Key words: 3T model, evapotranspiration, MODIS, Bowen ratio energy balance method

CLC number: P933 **Document code:** A

Citation format: Xiong Y J, Qiu G Y, Chen X H, Zhao S H and Tian F . 2012. Estimation of evapotranspiration using three-temperature model based on MODIS data. Journal of Remote Sensing, 16(5): 969–985

1 INTRODUCTION

Evapotranspiration (ET) is one of the key processes for hydrological cycle study. When water evaporating, it needs numerous energy, approximately accounting for 46% to 50% of solar energy absorbed by the earth surface (Trenberth, et al., 2009), making ET an important component of the energy balance. Therefore, the research on ET quantification has been watched closely by scientists in several fields such as remote sensing science, geography, hydrology and ecology (Sun, et al., 2009; Qiu & Zhao, 2010; Elhaddad, et al., 2011; Mo, et al., 2000; Xin, et al., 2003; Liu, et al., 2004; Xu, et al., 2004; Wang, et al., 2005; Wu, et al., 2008; Zhao, et al., 2008; Tian, et al., 2009; Pan & Liu, 2010), because ET is necessary for studies of climate change, crop water requirement in semiarid or arid areas, and regional sustainable water management practices.

The research on ET quantification has been conducted over 200 years ever since Dalton equation proposed in 1802, and many methods have been proposed to estimate ET, including Penman-Monteith (P-M) equation (Monteith, 1965), the Bowen ratio energy balance method (Bowen, 1926), eddy covariance (Swinbank, 1951) and lysimeter (Aboukhaled, et al., 1982). However, most of these methods are only appropriate for homogenous surfaces at micro scale (i.e.,from 0.1 km to 1 km), which is inadequate for water and heat balance. Since the late 1970s, remote sensing, especially the satellite remote sensing, has accelerated research on ET estimation, and physical based models have been established, such as SEBAL (surface energy balance algorithm for land) (Bastiaanssen, et al., 1998), two source models (Shuttleworth & Wallance, 1985; Mo, et al., 2004), N95 (Norman, et al., 1995; Zhang, et al., 2004) and triangle method (Carlson, 2007). SEBAL, METRIC (Allen, et al., 2007) and SEBS (Su, 2002; Jia, et al., 2003) are successed for some applications. In China, most researchs on ET quantification are focused on improvement of these three models and their applications, but new method to estimate ET is scarce.

Received: 2011-09-14; **Accepted:** 2012-01-19

Foundation: The Specialized Research Fund for the Doctoral Program of Higher Education of China (No.20110171120001); National Science Foundation for Post-doctoral Scientists of China (No.20090460795); National Natural Science Foundation of China (No.91025008, No.41101313); National Basic Research Program of China (973 Program) (No.2009CB421303)

First author biography: XIONG Yujiu (1982—), male, Ph.D., his research interest is remote sensing of the terrestrial water cycle. E-mail: xiongyuj@mail.sysu.edu.cn

The three-temperature (3T) model is a promising method to estimate ET. Based on the theory of surface energy balance and by introducing the reference sites, i.e., dry soil without evaporation (Qiu, et al., 1998) and a canopy without transpiration (Qiu, et al., 1996), algorithms to calculate the soil evaporation and the vegetation transpiration were proposed with advantages that aerodynamic resistance is eliminated and required few input parameters, whereas most of them can be retrieved from remote sensing data. Studies on field scale performed in the Arid Land Research Center, Tottori University, Japan showed that the overall error was less than 0.17 mm/d in terms of mean absolute error (Qiu, et al., 1996; 1998; 2002; 2006). However, the application of the 3T model for satellite based remote sensing has challenges in acquiring temperatures for dry soil and dry canopy (reference temperatures) when using satellite remote sensing, and dealing with evapotranspiration in mixed pixels as the 3T model is only suitable for estimating soil evaporation and vegetation transpiration. Considering these problems, we proposed primary solutions, and remote sensing application of the 3T model in a semi-arid grassland in Inner Mongolia, China showed that absolute error of the mean daily ET estimated by the 3T model and the observational data was 0.23 mm/d at 30 m spatial resolution (Xiong & Qiu, 2011).

The objective of this study is to further investigate remote sensing application of the 3T model at 1 km spatial resolution.

2 The 3T MODEL FOR SATELLITE BASED REMOTE SENSING

The 3T model for satellite based remote sensing includes three control algorithms, i.e., equations for soil evaporation (Eq. (1)), vegetation transpiration (Eq. (2)) and evapotranspiration (Eq. (3)), respectively. For application, the status of a pixel can be distinguished by the maximum and minimum thresholds of the normalized difference vegetation index (NDVI), and one of the three equations can be used to estimate ET.

$$LE_s = R_{n,s} - G_s - (R_{n,sd} - G_{sd})\frac{T_s - T_a}{T_{sd} - T_a},\ \mathrm{NDVI} \leqslant \mathrm{NDVI}_{min} \tag{1}$$

$$LE_c = R_{n,c} - R_{n,cp}\frac{T_c - T_a}{T_{cp} - T_a},\ \mathrm{NDVI} \geqslant \mathrm{NDVI}_{max} \tag{2}$$

$$L(\mathrm{ET}) = LE'_s + LE'_c,\ \mathrm{NDVI}_{min} < \mathrm{NDVI} < \mathrm{NDVI}_{max} \tag{3}$$

$$T_{sd} = \frac{R_{n,s} - G_s}{\rho_{air} C_P} r_a + T_a \tag{4}$$

$$T_{cp} = \frac{R_{n,c}}{\rho_{air} C_P} r_a + T_a \tag{5}$$

$$R_{n,r} = f(R_{swd}, \alpha_r, \varepsilon_r, T_r, T_a) \tag{6}$$

$$G_{sd} = f(R_{n,sd}) \tag{7}$$

where L is the latent heat of vaporization in W/(m^2 · mm) and E is evaporation or transpiration in mm; the subscripts s, c, sd and cp represent soil, vegetation canopy, the reference soil and the reference canopy respectively; R_n is the net radiation and G is the soil heat flux, both in W/m^2; T_a is the air temperature in K; ρ_{air} is the air density in kg/m^3; C_p is the specific heat of air at constant pressure; r_a is aerodynamic resistance in s/m; $R_{n,r}$ is net radiation absorbed by the reference soil or the reference canopy; R_{swd} stands for the incoming shortwave radiation; T_r stands for temperature of the reference soil or the reference canopy; α_r, ε_r are constants for surface albedo and land surface emissivity of the reference soil or the reference canopy, respectively (Xiong & Qiu, 2011).

It can be seen from Eq. (1) to Eq. (3) that there are five types of inputs in the 3T model, i.e., NDVI, net radiation, soil heat flux, land surface temperature (soil or canopy temperature), air temperature and parameters of reference sites. Among these inputs, except for air temperature which can be obtained and interpolated from meteorological stations, the others can be retrieved directly or indirectly from remote sensing data. Reference parameters can be estimated based on reference temperatures, which can be obtained using Eq. (4) and Eq. (5) and the aerodynamic resistance, calculated using methods adopted in SEBAL (Bastiaanssen, 2000). Net radiation can be estimated by combining R_{swd}, α_r, ε_r, reference temperatures and air temperature (Eq. (6)), and reference soil heat flux is strongly correlated with reference net radiation (Eq. (7)). A detailed description of the processes can be found in Xiong and Qiu (2011).

3 DATA SETS AND APPLICATION OF THE 3T MODEL

3.1 Study area

The study area locates in the Taibus Banner of Inner Mongolia, which is a typical agri-pasture transitional zone in the semi-arid region of Northern China. Cropland and pasture (including natural grassland and restored grassland) were the main land cover in this area, but vegetation cover was low. Zonal soil type was mainly chestnut soil and light chestnut soil, and soil texture was mainly sand and sandy loam. Topographic features of the area are mainly characterized by flat, with an elevation from 1300 m to 1800 m. The climate is continental, with a mean annual temperature, precipitation and pan evaporation of 1.6 °C, 407 mm and 1900 mm, respectively.

The field experiment was conducted in Farmland and Grassland Ecosystem Observation Station of Beijing Normal University. Three observation stations, monitoring water budget, were selected (Fig. 1). Observational items of each station included soil heat flux (G) at 1 cm and 5 cm respectively below the ground surface, and routine meteorological factors overground at two different heights, i.e., net radiation (R_n) and wind speed at 2 m height, and air temperature and humidity measured at 1.5 m and 2 m height respectively. All data were collected by a data-logger (model DT500 series 3) every five seconds and ten minutes averages were calculated and stored. System 1 measured precipitation additionally, but unfortunately there was no more interface for installing net radiation and soil heat flux. Thus there were only two Bowen ratio systems (BRS) (Fig. 1).

3.2 Datasets and processing

In this study, datasets included observational data from BRS, remote sensing data and geospatial data.

The BRS began operating on June 12, 2008 and stopped at the end of 2009. The observational data was used to calculate instantaneous evapotranspiration (mean value of each ten minutes) through

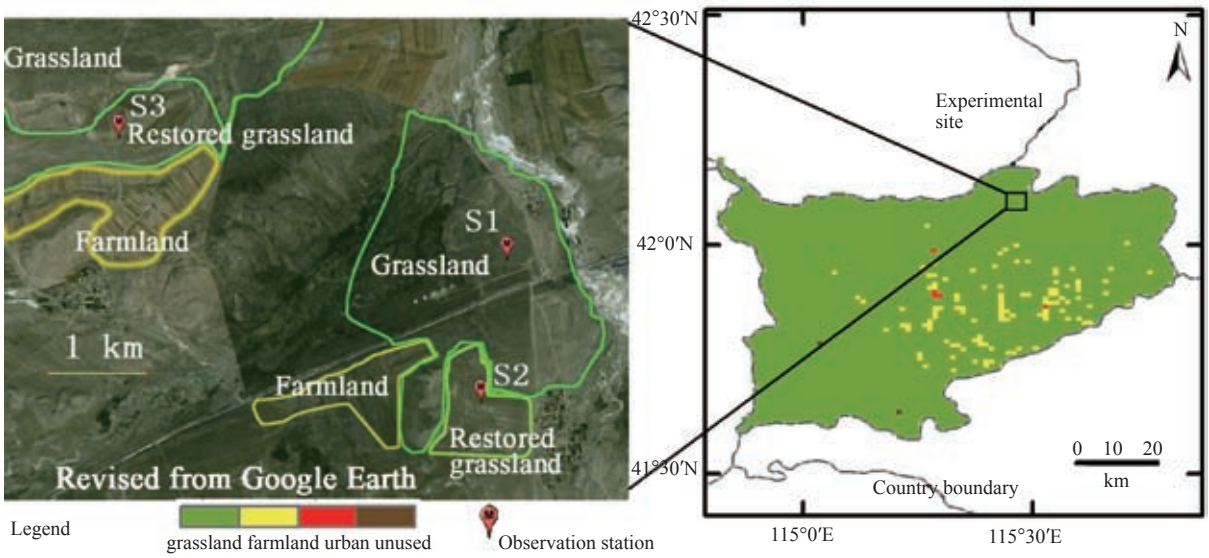

Fig. 1 Location of the experimental site

Bowen ratio energy balance method (BREBM, Eq. (8) and Eq. (9)), and daily evapotranspiration (ET_β) (from sun rise to sun set) was calculated by sum instantaneous values.

$$\beta = \frac{C_p \Delta T}{L \Delta q} = \frac{C_p P \Delta T}{L \varepsilon_{\text{ratio}} \Delta e_a} = \frac{C_p P (T_{1.5} - T_{2.0})}{L \varepsilon_{\text{ratio}} (e_{1.5} - e_{2.0})} \quad (8)$$

$$LE = \frac{R_n - G}{\beta + 1} \quad (9)$$

where β is the Bowen ratio, which is valid between –0.7 and 10 since the BREBM results in unreliable estimation when β approaches –1 and larger than 10 (Andreas & Cash, 1996; Pauwels & Samson, 2006); C_p is the air heat capacity at constant pressure; ΔT, Δq and Δe_a are air temperature difference, humidity difference, and water vapor pressure difference (see FAO irrigation and drainage in paper 56 for calculation (Allen, et al., 1998)) between the upper and lower air layers, respectively; T is the air temperature; the subscripts 1.5 and 2.0 represent two different heights; R_n and G are the measured net radiation and soil heat flux, respectively; and $\varepsilon_{\text{ratio}}$ is the ratio of the molecular weight of water vapour to dry air (approximately equals to 0.622).

Remote sensing data included MODIS L1B image and MODIS land use product (MCD12Q1, Fig. 1). According to the NASA, eleven MODIS L1B images without cloud impact or affected little by the cloud were selected during the observation (Table 1). Nine bands (i.e., from band 1 to band 5, band 7, band 19, band 31 and band 32) and auxiliary information (i.e., solar zenith angle, latitude and longitude) needed as the model input were extracted and processed to 1 km spatial resolution with UTM projection (WGS84, UTM zone 50N) using MODIS Conversion Toolkit in ENVI software.

Geospatial data included DEM and vector data of administrative boundaries. DEM, obtained from the Consortium for Spatial Information (CGIAR-CSI), has a resolution of 90 m. All the geospatial data was preprocessed and projected to the coordinate system with spatial resolution the same as the processed MODIS L1B images.

Table 1 Information of the adopted MODIS L1B data

Satellite	Acquisition date and scan time(UTC)	DOY	Satellite	Acquisition date and scan time(UTC)	DOY
Terra	2008-07-12 3:40	194	Terra	2008-09-02 3:15	246
Terra	2008-07-23 3:20	205	Terra	2008-09-18 3:16	262
Aqua	2008-07-29 6:05	211	Terra	2008-10-03 2:30	277
Aqua	2008-08-03 4:45	216	Terra	2008-10-11 3:20	285
Aqua	2008-08-05 4:30	218	Terra	2008-10-12 2:25	286
Aqua	2008-08-14 5:20	226			

Note:day of year (DOY)

3.3 Evapotranspiration retrieval method

While applying the 3T model, soil temperature and canopy temperature were estimated using Eq. (10) (Lhomme, et al., 1994) and MODIS land surface temperature retrieved from split-window method (Sobrino & Raissouni, 2000). The status of a MODIS pixel was distinguished according to Sobrino, et al. (2003), i.e., when a pixel's NDVI was less than 0.2, it was assumed to be a bare soil pixel. Pixels with NDVI values larger than 0.5 were assumed to be vegetated pixels. For the NDVI between 0.2 and 0.5, it was supposed to be a mixture of soil and vegetation. Methods to estimate other input parameters can be found in Xiong and Qiu (2011). When all the necessary inputs for the 3T model were available, the instantaneous ET rate was estimated; thereafter daily ET was derived using the method proposed by Jackson, et al. (1983).

$$\begin{aligned} T_{\text{s,MODIS}} &= fT_c + (1-f)T_s \\ T_s - T_c &= a(T_{\text{s,MODIS}} - T_a)^m \end{aligned} \quad (10)$$

where f is fractional vegetation cover; $T_{\text{s, MODIS}}$ is the retrieved MODIS land surface temperature; a and m are empirical coefficients. The values a = 0.1 and m = 2 were used in this paper (Xiong & Qiu, 2011).

4 RESULTS AND DISCUSSION

4.1 Daily ET retrieved from the 3T model

Using the 3T model, daily ET was estimated based on the MODIS L1B images and the results are shown in Fig. 2. Statistical results showed that the modeled ET varied from 1.28 mm/d to 9.03 mm/d in the growing season, with a mean value of 4.58 mm/d. Temporally, ET value increased first and then decreased gradually as the evolving of the growing season (Fig. 3), which was consistent with the observed data. Spatially, the modeled daily ET distributed homogeneously, and ET value in the same day showed little difference in October (from Fig. 2(i) to Fig. 2 (k)), but it varied in other months (from Fig. 2(a) to Fig. 2(h)).

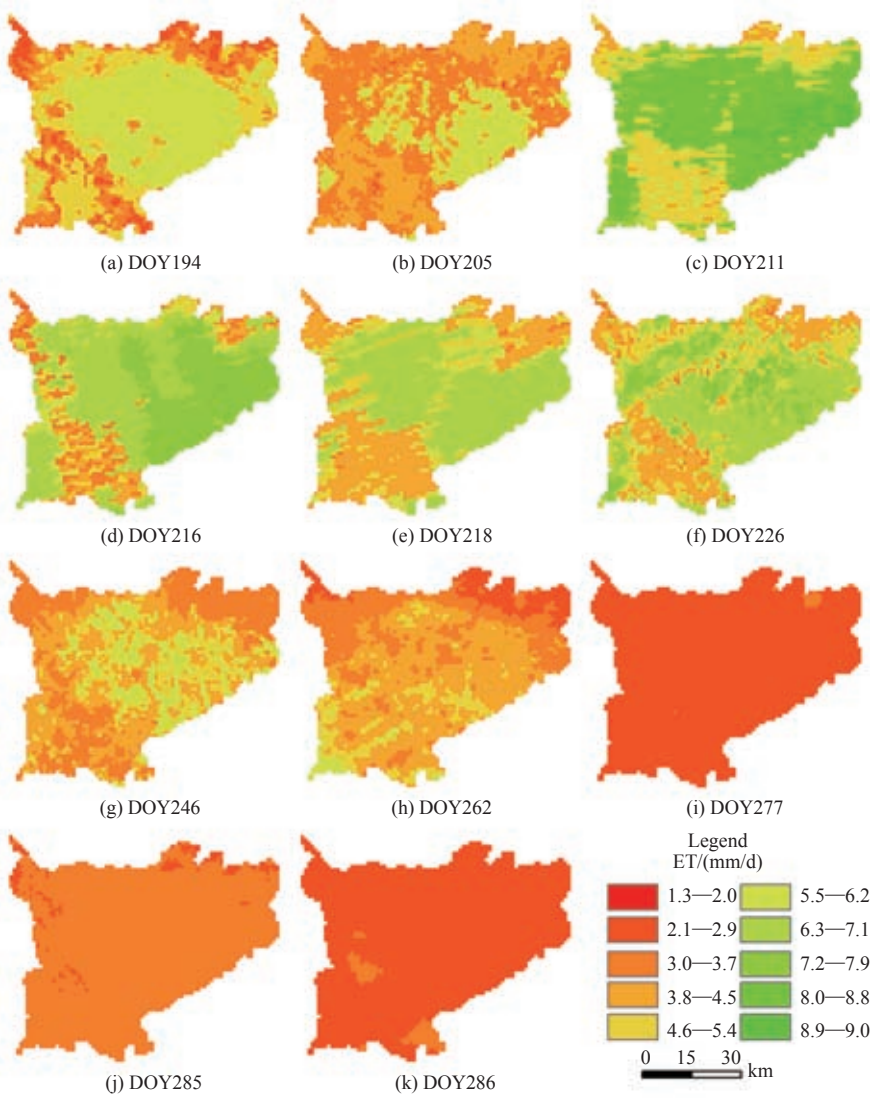

Fig. 2 Daily ET retrieved from the 3T model based on 1 km MODIS data in 2008

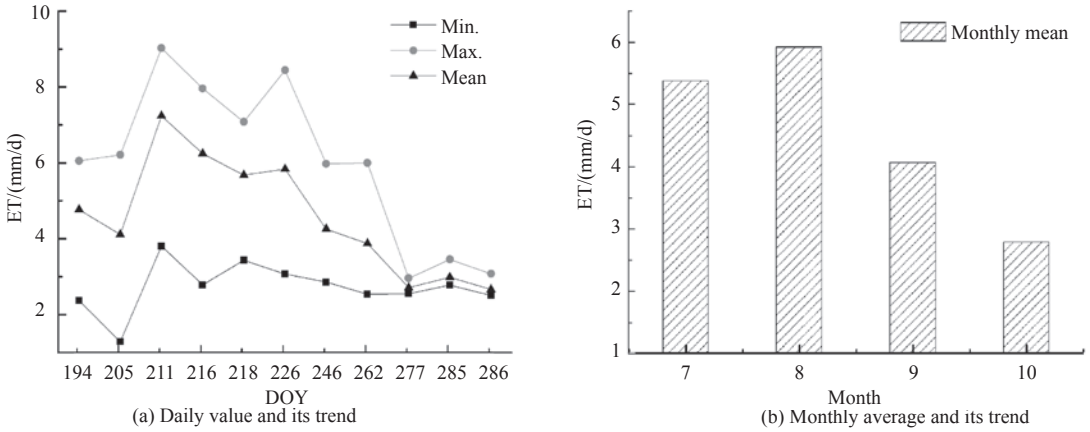

Fig. 3 Statistical results of the modeled ET

4.2 Model validation

The modeled daily ET was averaged within block sizes of 3×3 pixels around the center of the BRS and then compared with the ET calculated by using the BREBM. The mean absolute error (MAE) and the mean absolute percent error (MAPE) were used to assess the model performance during the evaluation process.

As shown in Table 2, the MAE between the modeled daily ET and the observational data was 0.72 mm/d, with maximum and minimum absolute errors of 2.78 mm/d and 0.11 mm/d, respectively. When comparing results of the two BRS, accuracy of the 3T model in BRS 2 was higher than that of BRS 3, because the MAE for BRS 2 was 0.64 mm/d with maximum and minimum absolute errors of 2.78 mm/d and 0.11 mm/d, respectively, whereas it was 0.80 mm/d for BRS 3 with maximum and minimum absolute errors of 1.64 mm/d and 0.11 mm/d, respectively.

As shown in Table 3, the MAPE between the modeled daily ET and the observational data was 20.76%. If the MAPE was classified into four levels, i.e., less than 0. 1 (level 1), less than 0.2 and greater than 0.1 (level 2), less than 0.3 and greater than 0.2 (level 3), and greater than 0.3 (level 4), the first three levels accounted for 47.6%, 19.1% and 9.5%, respectively (Table 3).

Table 2 Validation of the modeled daily ET with in-situ measurements

DOY	Bowen ratio system 2				Bowen ratio system 3			
	ET_β /mm	ET_M /mm	AE /mm	APE /%	ET_β /mm	ET_M /mm	AE /mm	APE /%
194	5.96	3.18	2.78	46.64	3.15	3.31	0.16	5.08
205	3.60	4.19	0.59	16.39	2.50	3.84	1.34	53.60
211	5.44	5.20	0.24	4.41	4.62	4.48	0.14	3.03
216	5.45	6.68	1.23	22.57	5.11	5.97	0.86	16.83
218	4.66	4.88	0.22	4.72	4.40	5.03	0.63	14.32
226	4.59	4.96	0.37	8.06	3.97	4.34	0.37	9.32
246	3.09	3.27	0.18	5.83	3.14	3.25	0.11	3.50
262	2.60	2.83	0.23	8.85	2.15	2.76	0.61	28.37
277	2.71	2.82	0.11	4.06	1.18	2.75	1.57	133.05
285	—	2.94	—	—	1.25	2.89	1.64	131.20
286	2.18	2.60	0.42	19.27	1.23	2.58	1.35	109.76
Mean	4.03		0.64	15.81	2.97		0.80	26.80
	MAE 0.72 mm				MAPE 20.76%			

Note: ET_β represents ET deduced by the Bowen ratio systems; ET_M represents ET estimated by the 3T model; — Observational data was abnormal

$$AE=|ET_\beta - ET_M|$$

$$APE=|ET_\beta - ET_M|/ET_\beta$$

$$MAE=\sum(|ET_\beta - ET_M|)/n$$

$$MAPE=(100/\overline{ET_\beta})\sum(|ET_\beta - ET_M|)/n$$

Table 3 Statistical results of MAPE with different standards

MAPE	Statistics based on single BRS/%		Statistics based on two BRSs /%
	2	3	
<0.1	60.0	36.4	47.6
<0.2	20.0	18.2	19.1
<0.3	10.0	9.1	9.5
≥0.3	10.0	36.3	23.8

4.3 Discussion

In this section, accuracy evaluation would be discussed according to APE by analyzing daily observational data.

There were 16 APEs less than 0.3 (Table 2), and data on DOY 218 observed from BRS 3 was selected as a representation because its APE was 14.32%, nearly half of 30%. Fig. 4 (a) shows the observed net radiation, soil heat flux and latent heat flux on DOY 218 at BRS 3, and it was clear that the observed data changed smoothly, indicating that ET calculated using the BREBM was reasonable and the validation results were authentic.

For BRS 2, APE on DOY 194 was greater than 0.3. As shown in Fig. 4 (b), latent heat flux calculated using the BREBM was greater than observed net radiation from 6:00 to 14:00 and almost equal to net radiation in the rest of the time, suggesting ET calculated by using the BREBM was incorrect.

For BRS 3, APEs on DOY 205, DOY 277, DOY 285 and DOY 286 were greater than 0.3. On DOY 205, observational data declined dramatically after 12 (Fig. 4 (c)), indicating an abnormal observation. DOY 285 was chosen as a representation for DOY 277 and DOY 286, and the observational data was shown in Fig. 4 (d). It was clear the observation was normal, suggesting ET calculated by using the BREBM was reasonable.

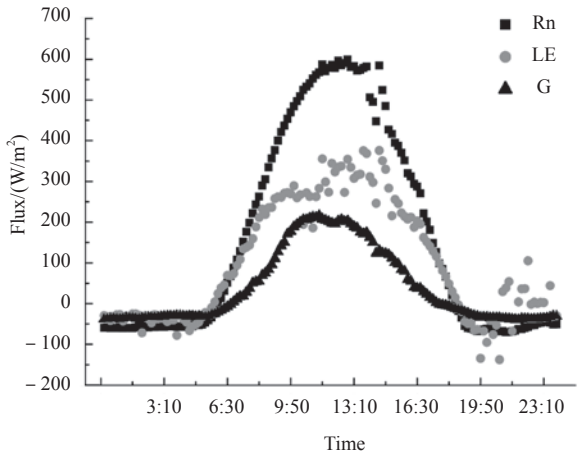

(a) System 3 on DOY 218

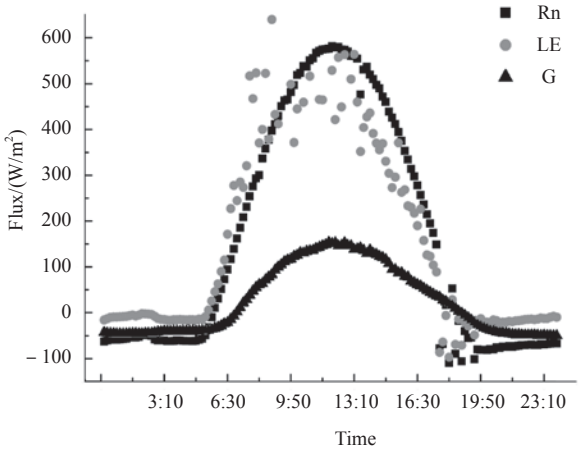

(b) System 2 on DOY 194

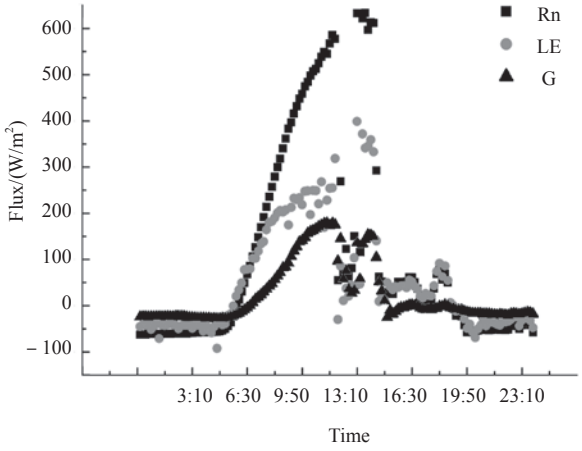

(c) System 3 on DOY 205

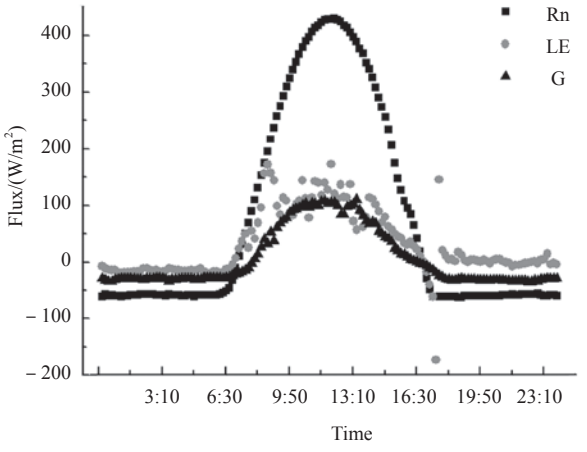

(d) System 3 on DOY 285

Fig. 4 Daily observational data of Bowen ratio systems

Overall, except two abnormal observations, the other 19 observed data were authentic, indicating the calculated ET values were correct, which were also proved by water budget experiments performed in the same period and location (Qiu, et al., 2011). Considering these 19 valid validations, the MAE between the modeled daily ET and the observational data was 0.58 mm/d, with maximum and minimum absolute errors of 1.64 mm/d and 0.11 mm/d, respectively. The paired ET was further plotted on a scatter diagram, in which most points distributed closely along the 1:1 line (Fig. 5).

There might be some uncertainty in the validation due to two reasons. One is the coarse resolution of MODIS data, which could not effectively reflect the nuances of earth surface, such as ET values observed in the same day in October showed significant difference. But the modeled ET showed little difference (Table 2) even distance between the two stations was only 4.5 km. And observational area of BRS was less than 1 km^2 (Baldocchi, 2003; Rana & Katerji, 2000), but mean value of 3×3 pixels represented 9 km^2 was adopted, comparing between these two scales might lead to uncertainty.

It is suggested the closer of the energy closure ratio (ECR) of a flux tower to 1, the smaller the deviation between the observed and modeled ET (Wu, et al., 2008). Results showed ECR was 0.9 in a grassland from May to September in Xikin Gol (Yue, et al., 2010), northeast of the study area. Assuming ECR of the study area was 0.9,

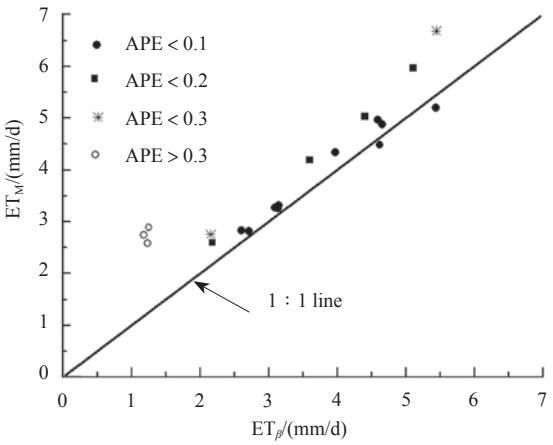

Fig. 5 Scatter diagram of daily ET estimated by the 3T model (ET_M) and the RMEBE (ET_β)

our validation results were promising.

5 CONCLUSION

Observation data, obtained from two Bowen ratio systems between July and October in 2008 in a semi-arid grassland in Taibus Banner of Inner Mongolia, China were used to validate daily ET estimated by the 3T model at 1 km spatial resolution. The key points of this study were as below. (1) In the adopted 22 observational data, 19 ET values calculated by the Bowen ratio energy balance method were authentic. (2) ET estimated using the 3T model and MODIS L1B data varied from 1.28 mm/d to 9.03 mm/d in the growing season, with a mean value of 4.58 mm/d. (3) Validation results showed that the mean absolute error between the observed and modeled ET was 0.58 mm/d, with maximum and minimum absolute errors of 1.64 mm/d and 0.11 mm/d respectively, and the mean absolute percent error was 17.10%.

Acknowledgements: Thanks to Xie Fang, Wang Pei and Feng Youcan, for their work, and to the NASA for providing MODIS data. We also thank the fruitful comments by the editors and anonymous reviewers.

REFERENCES

Aboukhaled A, Alfaro A and Smith M. 1982. FAO Irrigation and Drainage Paper No. 39, Lysimeters. Rome: FAO

Allen R G, Pereira L S, Raes D and Smith M. 1998. FAO Irrigation and drainage paper No. 56, Crop evapotranspiration-Guidelines for computing crop water requirements. Rome: FAO

Allen R G, Tasumi M, Morse A, Trezza R, Wright J L, Bastiaanssen W, Kramber W, Lorite I and Robison C W. 2007. Satellite-based energy balance for mapping evapotranspiration with internalized calibration (METRIC)-applications. Journal of Irrigation and Drainage Engineering, 133(4): 395–406 [DOI: 10.1061/(ASCE)0733-9437(2007)133:4(395)]

Andreas E L and Cash B A. 1996. A new formulation for the Bowen ratio over saturated surfaces. Journal of Applied Meteorology, 35(8): 1279–1289 [DOI: 10.1175/1520-0450-(1996)035<1279:ANFFTB>2.0.CO;2]

三温模型与MODIS影像反演蒸散发

熊育久[1,2]，邱国玉[3]，陈晓宏[1,2]，赵少华[4]，田菲[5]

1. 中山大学 地理科学与规划学院水资源与环境系，广东 广州 510275;
2. 中山大学华南地区水循环与水安全广东省普通高校重点实验室，广东 广州 510275;
3. 北京大学 深圳研究生院环境与能源学院，广东 深圳 518055;
4. 环境保护部 卫星环境应用中心，北京 100094;
5. 北京师范大学 资源学院，北京 100875

摘　要：提出三温模型结合MODIS数据反演区域蒸散发的方法，在内蒙古草原开展案例研究，以2008年植被生长季(7—10月)的波文比系统观测数据为标准，对该方法进行检验。结果表明：三温模型反演的蒸散发量，平均值、最大、最小值分别为4.58 mm/d、9.03 mm/d、1.28 mm/d；蒸散发反演结果在空间上分布较均匀，与草原的均一性相吻合，在时间上蒸散发的数值先逐渐增大，8月后逐渐减小，与观测结果相一致；三温模型反演的蒸散发量与观测值之间的最小、最大绝对误差分别为0.11 mm/d、1.64 mm/d，平均绝对误差为0.58 mm/d、平均相对误差为17.10%。三温模型在1 km空间尺度的反演精度较理想。

关键词：三温模型，蒸散发，MODIS，波文比能量平衡法

中图分类号：P933　　**文献标志码**：A

引用格式：熊育久，邱国玉，陈晓宏，赵少华，田菲. 2012. 三温模型与MODIS影像反演蒸散发. 遥感学报，16(5): 969–985
Xiong Y J, Qiu G Y, Chen X H, Zhao S H and Tian F . 2012. Estimation of evapotranspiration using three-temperature model based on MODIS data. Journal of Remote Sensing, 16(5): 969–985

1　引　言

蒸散发ET(Evapotranspiration)是水分循环中的关键环节之一，其形成过程中吸收的能量可占地表吸收太阳能的46%—50% (Trenberth 等，2009)，亦是地表能量平衡的重要组成部分。蒸散发定量估算是水热平衡研究的重点，对干旱/半干旱地区的植被/作物需水及水资源管理、气候变化等领域具有重要意义，一直是遥感科学、地理学、水文学和生态学等关注的焦点(莫兴国 等，2000；辛晓洲 等，2003；刘绍民 等，2004；徐新良 等，2004；王庆改 等，2005；吴炳方 等，2008；赵长森 等，2008；Sun 等，2009；田静 等，2009；潘竟虎和刘春雨，2010；Qiu和Zhao，2010；Elhaddad 等，2011)。

自1802年Dalton提出计算蒸发的公式以来，蒸散发定量研究已有200多年的历史，一系列计算方法被相继提出，如Penman-Monteith公式(Monteith，1965)、波文比能量平衡法(Bowen，1926)、涡度相关法(Swinbank，1951)、蒸渗仪法(Aboukhaled 等，1982)。然而，这些传统方法应用多局限在0.1—1 km尺度(Rana和Katerji，2000；Baldocchi，2003)和平坦均匀的下垫面(Scott 等，2000)，难以满足区域尺度研究水热平衡的需求。20世纪70年代以来，卫星遥感技术的出现和发展促进了蒸散发遥感估算研究，先后提出一些具有物理基础意义的模型，如单层模型SEBAL(Bastiaanssen 等，1998)、系列模式双层模型(Shuttleworth和Wallance，1985；Mo 等，2004)、平行模式双层模型(Norman 等，1995；张仁华 等，2004)、温度－植被指数空间关系模型(Carlson，2007)。其中，成功用于定量估算区域蒸散发的模

收稿日期：2011-09-14；**修订日期**：2012-01-19

基金项目：高等学校博士学科点专项科研基金(编号: 20110171120001)；中国博士后科学基金项目(编号: 20090460795)；国家自然科学基金项目(编号: 91025008，41101313)；国家重点基础研究发展计划(973计划)(编号: 2009CB421303)。

第一作者简介：熊育久(1982—)，男，博士，讲师，主要从事蒸散发遥感反演与应用研究。E-mail: xiongyuj@mail.sysu.edu.cn。

型，以SEBAL及基于类似原理的METRIC模型(Allen 等，2007)、SEBS 模型(Su，2002；Jia 等，2003)为主。国内研究主要集中在对这些模型的改进与应用，新的计算方法很少见。

三温模型(3T model)是近年提出的一种计算蒸散发的新方法，该模型以地表能量平衡方程为基础，通过引入参考土壤(干燥、无蒸发的土壤)(Qiu 等，1998)和参考植被(干燥、无蒸腾的植被)(Qiu 等，1996)，剔除难以准确计算的空气动力学阻抗，推导出土壤蒸发子模型和植被蒸腾子模型，其主要优点是不需要动力学阻抗、输入参数较少、大多参数可通过遥感数据提取。自三温模型提出后，在日本鸟取大学干燥地研究中心的实验地开展了大量田间尺度研究，结果表明模型操作简便、模拟误差仅有0.17 mm/d (Qiu 等，1996，1998，2002，2006)。若要将三温模型应用于区域尺度，虽然气温可利用气象观测资料，净辐射、土壤热通量、植被温度、土壤温度等参数可通过遥感方法估算，但参考土壤、参考植被的参数在田间尺度可实测获得，在大尺度应用时难以实现。此外，三温模型中的土壤蒸发、植被蒸腾子模型只适用相应的纯净像元，但遥感数据中绝大部分像元是地面多种信息的混合体(混合像元)，如何计算混合像元的蒸散发亟待解决。针对三温模型在区域大尺度应用中面临的难题，本文作者提出初步解决方案，在内蒙古草原开展了案例研究，结果表明：在30 m空间尺度下，基于遥感的三温模型反演的蒸散发，与观测值的绝对误差仅为0.23 mm/d (Xiong和Qiu，2011)。

本研究的目的是深入讨论三温模型的遥感应用，通过实验观测数据进行验证，利用波文比系统观测资料，结合同步MODIS遥感数据，检验三温模型在1 km空间尺度的精度，为区域蒸散发定量研究提供一种新方法。

2 基于遥感的三温模型介绍

基于遥感的三温模型，包括土壤蒸发子模型(式(1))、植被蒸腾子模型(式(2))和蒸散发子模型(式(3))。在应用时，根据植被指数(NDVI)的最大、最小阈值，将下垫面在遥感影像中的属性归结为纯净像元与混合像元，对纯净土壤像元，直接利用三温模型中土壤蒸发子模型；对纯净植被像元，直接利用植被蒸腾子模型；对混合像元，分别计算其土壤蒸发、植被蒸腾后求和。

$$LE_s = R_{n,s} - G_s - (R_{n,sd} - G_{sd})\frac{T_s - T_a}{T_{sd} - T_a},\ \mathrm{NDVI} \leqslant \mathrm{NDVI}_{min} \quad (1)$$

$$LE_c = R_{n,c} - R_{n,cp}\frac{T_c - T_a}{T_{cp} - T_a},\ \mathrm{NDVI} \geqslant \mathrm{NDVI}_{max} \quad (2)$$

$$L(\mathrm{ET}) = LE'_s + LE'_c,\ \mathrm{NDVI}_{min} < \mathrm{NDVI} < \mathrm{NDVI}_{max} \quad (3)$$

$$T_{sd} = \frac{R_{n,s} - G_s}{\rho_{air} C_P} r_a + T_a \quad (4)$$

$$T_{cp} = \frac{R_{n,c}}{\rho_{air} C_P} r_a + T_a \quad (5)$$

$$R_{n,r} = f(R_{swd}, \alpha_r, \varepsilon_r, T_r, T_a) \quad (6)$$

$$G_{sd} = f(R_{n,sd}) \quad (7)$$

式中，L是水汽汽化潜热(W/(m^2 · mm))，E_s是土壤蒸发(mm)，$R_{n,s}$是土壤吸收的太阳净辐射(W/m^2)，G_s是土壤热通量(W/m^2)，$R_{n,sd}$是参考土壤吸收的太阳净辐射(W/m^2)，G_{sd}是参考土壤热通量(W/m^2)，T_s是土壤温度(K)，T_{sd}是参考土壤温度(K)，T_a是气温(K)，E_c是植被蒸腾(mm)，$R_{n,c}$是植被吸收的太阳净辐射(W/m^2)，$R_{n,cp}$是参考植被吸收的太阳净辐射(W/m^2)，T_c是植被冠层温度(K)，T_{cp}是参考植被温度(K)，ET是混和像元的蒸散发(mm)，E'_s、E'_c分别代表混和像元中的土壤蒸发与植被蒸腾，ρ_{air}是空气密度，C_p是空气定压比热，r_a是空气动力学阻抗(s/m)，$R_{n,r}$是参考面吸收的太阳净辐射，R_{swd}为短波辐射(W/m^2)，T_r代表参考温度，α_r、ε_r分别是参考面的反照率、比辐射率(均为常数(Xiong和Qiu，2011))。

由式(1)—式(3)可知，基于遥感的三温模型输入参数共5类，包括：净辐射、土壤热通量、地表温度(土壤表面温度与植被冠层温度)、气温、参考面参数(参考净辐射、参考土壤热通量、参考地表温度)、NDVI。其中：净辐射、土壤热通量、地表温度、NDVI均可通过遥感数据直接或间接反演获得，且均有比较成熟的反演算法；气温通常可由气象站点观测资料插值。本文作者初步提出了以参考地表温度为核心的参考参数遥感获取方法，即：参考温度是某像元达到无蒸发或无蒸腾时所具有的理论温度，据此，令能量平衡方程中的蒸散发项为零，可推导出参考温度的计算式(4)以及式(5)，其中阻抗的计算采用SEBAL的算法(Bastiaanssen，2000)(阻抗被引入，剔除阻抗、改进参考地表温度的算法是进一步研究重点)；净辐射是地表温度、地表反照率、地

表比辐射率等的函数(式(6))，因此用参考温度替换地表温度，并将地表反照率、比辐射率赋予干燥土壤或干燥植被的特定值，可计算出参考净辐射；土壤热通量是净辐射的函数(式(7))，因此可根据参考净辐射计算参考土壤热通量。具体内容请参考文献Xiong和Qiu (2011)。

3 数据处理与蒸散发反演

3.1 研究区自然概况

研究区位于内蒙古自治区锡林郭勒盟西南部的太仆寺旗境内，是中国北方典型的干旱、半干旱农牧交错生态脆弱带。下垫面主要是耕地和草地(包括原生草地与退耕草地，代表群系为大针茅草和羊草)，土壤有机质含量低，土壤较贫瘠，质地较粗，颗粒组成以中粗砂为主(占50%以上)，植被覆盖率较低。太仆寺旗地形较平坦(海拔在1300—1800 m)，年平均气温较低，仅有1.6℃；受蒙古高压气团控制，全年多西北风，年均风速3.41 m/s，最大值高达20 m/s；太仆寺旗年降水量少，为407 mm，多集中在7月、8月、9月，占全年总降水量的65%，但其年均蒸发量却高达1900 mm。

地面观测地点设在太仆寺旗的农田－草地生态系统国家野外站。在野外站附近选取具有代表性的平坦下垫面建立波文比系统观测场，观测研究不同下垫面(包括原生草地、退耕草地、耕地，见图1)的水分收支。最终建立3处波文比系统观测场，各由一套DT500系列3自动气象站构成，观测项目包括2 m高度处的太阳总辐射、净辐射、风速、风向、温度、湿度，1.5 m高度处的气温和湿度，以及土壤热通量(距地表1 cm、5 cm两个不同深度)。自动气象站以太阳能驱动，自动观测和记录，数据记录间隔为10 min。1号自动气象站还有降水观测，但能量观测只有太阳总辐射，数据采集器已无接口再安装净辐射传感器与土壤热通量传感器，因此仅有2、3号气象站构成波文比观测系统(图1)。

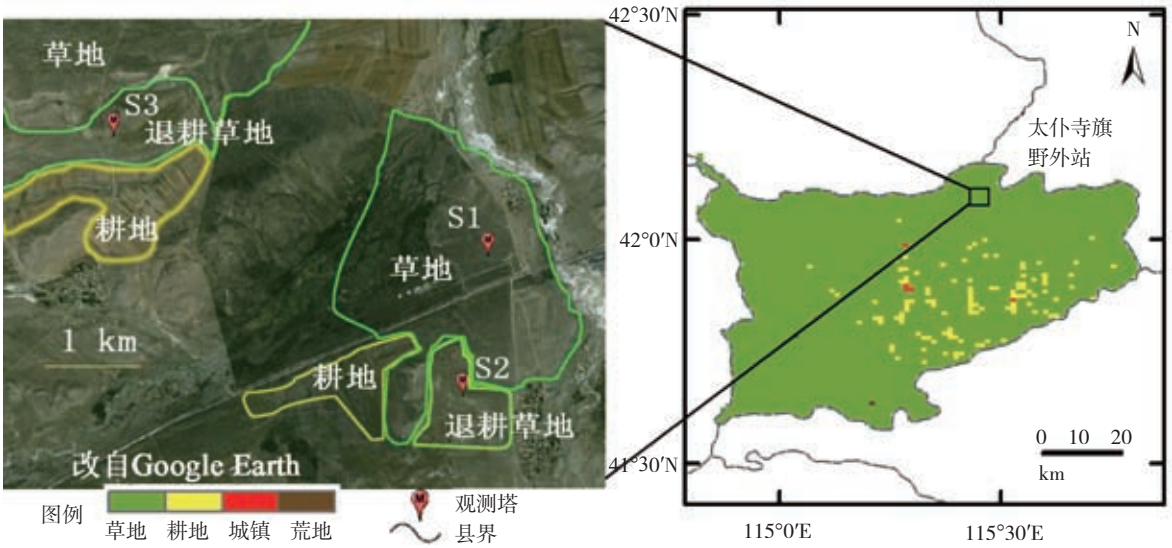

图 1 内蒙古太仆寺旗土地利用类型及观测塔地理位置

3.2 数据处理

本文采用的资料包括波文比系统观测资料、遥感数据、基础空间地理数据。

波文比系统观测时间从2008年7月至2009年。蒸散发利用波文比能量平衡法计算(式(8)(9))，即根据两个不同高度的温湿度差值之比计算波文比值，再计算每10 min的平均蒸散发。日蒸散发量(ET)用日出至日落期间每10 min的瞬时值累加，其中需剔除波文比值＜－0.7或＞10.0的错误结果(Andreas和Cash，1996；Pauwels和Samson，2006)，剔除造成的数据缺失采用邻近数据线性内插。

$$\beta=\frac{C_p\Delta T}{L\Delta q}=\frac{C_pP\Delta T}{L\varepsilon_{\text{ratio}}\Delta e_a}=\frac{C_pP\left(T_{1.5}-T_{2.0}\right)}{L\varepsilon_{\text{ratio}}\left(e_{1.5}-e_{2.0}\right)} \quad (8)$$

$$LE=\frac{R_n-G}{\beta+1} \quad (9)$$

式中，β是波文比，C_p是空气定压比热(MJ/(kg · ℃))，

ΔT是不同高度的气温差(℃)，Δq是不同高度的湿度差，P是大气压(kPa)，ε_{ratio}是水汽和干空气的分子量比值(约为0.622)，Δe_a是不同高度的实际水汽压差(kPa)，其计算方法请参考FAO irrigation and drainage paper 56 (Allen 等，1998)，下标1.5和2.0分别代表高度(m)，LE是潜热通量，R_n、G分别是净辐射、土壤热通量，均有观测结果。

遥感数据采用MODIS L1B影像。结合波文比系统观测日期，根据NASA发布的MODIS真彩色合成影像，选择不受云影响或影响不大的11次过境数据(表1)。在分析中应用了2008年的MODIS土地覆盖产品MCD12Q1(图1)。在处理数据时，提取反演中所需的9个波段(第1、2、3、4、5、7、19、31、32波段)，以及太阳天顶角、经纬度等附加信息，利用ENVI软件中的MODIS Conversion Toolkit插件对数据投影转换，生成空间分辨率为1 km的UTM(WGS84、UTM zone 50N)影像。

表1 采用的MODIS L1B影像信息

卫星	过境日期与时间(UTC)	DOY	卫星	过境日期与时间(UTC)	DOY
Terra	2008-07-12 3:40	194	Terra	2008-09-02 3:15	246
Terra	2008-07-23 3:20	205	Terra	2008-09-18 3:16	262
Aqua	2008-07-29 6:05	211	Terra	2008-10-03 2:30	277
Aqua	2008-08-03 4:45	216	Terra	2008-10-11 3:20	285
Aqua	2008-08-05 4:30	218	Terra	2008-10-12 2:25	286
Aqua	2008-08-14 5:20	226			

注：DOY表示一年中的第几天

基础空间地理数据包括数字高程模型(DEM)数据、矢量行政边界等。DEM空间分辨率90 m，来源于国际农业研究咨询组织(CGIAR)的空间信息联盟(CSI)。矢量行政边界来源于国家地理信息中心。经坐标投影转换处理，全部投影到UTM(WGS84、UTM zone 50N)坐标系，确保地理数据与处理的遥感影像坐标系统一致，并将DEM重采样到1 km空间分辨率。

3.3 蒸散发反演

三温模型中所需的土壤表面温度与植被冠层温度可根据Lhomme等人(1994)提出的算法(式(10))，从反演的MODIS地表温度求解。纯净土壤像元、纯净植被像元和混和像元根据Sobrino等人(2003)提出的NDVI阈值确定，即：当MODIS像元的NDVI<0.2时，该像元为纯净土壤；当MODIS像元的NDVI>0.5时，该像元为纯净植被；NDVI介于0.2—0.5之间时为混和像元。MODIS地表温度采用Sobrino和Raissouni(2000)的劈窗算法反演。净辐射、土壤热通量及参考参数的详细反演方法请参见文献(Xiong和Qiu，2011)，本文不再赘述。三温模型反演的瞬时蒸散发，根据Jackson等人(1983)的方法积分到日尺度。

$$T_{s,MODIS} = fT_c + (1-f)T_s$$
$$T_s - T_c = a(T_{s,MODIS} - T_a)^m \quad (10)$$

式中，f是植被盖度；$T_{s,MODIS}$为MODIS地表温度，a和m是经验系数，本文取a = 0.1、m = 2 (Xiong和Qiu，2011)。

4 反演结果与分析

4.1 日蒸散发量反演结果

图2是三温模型反演的蒸散发结果。基于同期无云的11天MODIS L1B影像反演的蒸散发量，在2008年生长季的平均值、最大、最小值分别为4.58 mm/d、9.03 mm/d、1.28 mm/d。在空间上，各天的蒸散发量分布相对均一，在生长季中7月、8月、9月各日的数值差异相对明显(图2(a)—(h))，但在10月份差异不大(图2(i)—(k))，这与草原下垫面相对均匀是一致的。从时间上，经统计，蒸散发量大致呈先增加再逐渐减小的趋势，即7月、8月份是植被生长旺季，下垫面的蒸散发数值逐渐增大，在8月达最大值，然后随着生长季的结束逐渐减小(图3)，该结论与波文比系统观测的结果相一致。

4.2 模型反演精度分析

以波文比系统为中心，取3 × 3像元均值代表反演结果，以观测数据和波文比能量平衡法计算的蒸散发量为标准，验证本文模型反演的结果(见表2、表3)。验证中采用绝对误差、相对误差评价反演的蒸散发量与观测值之间的关系。

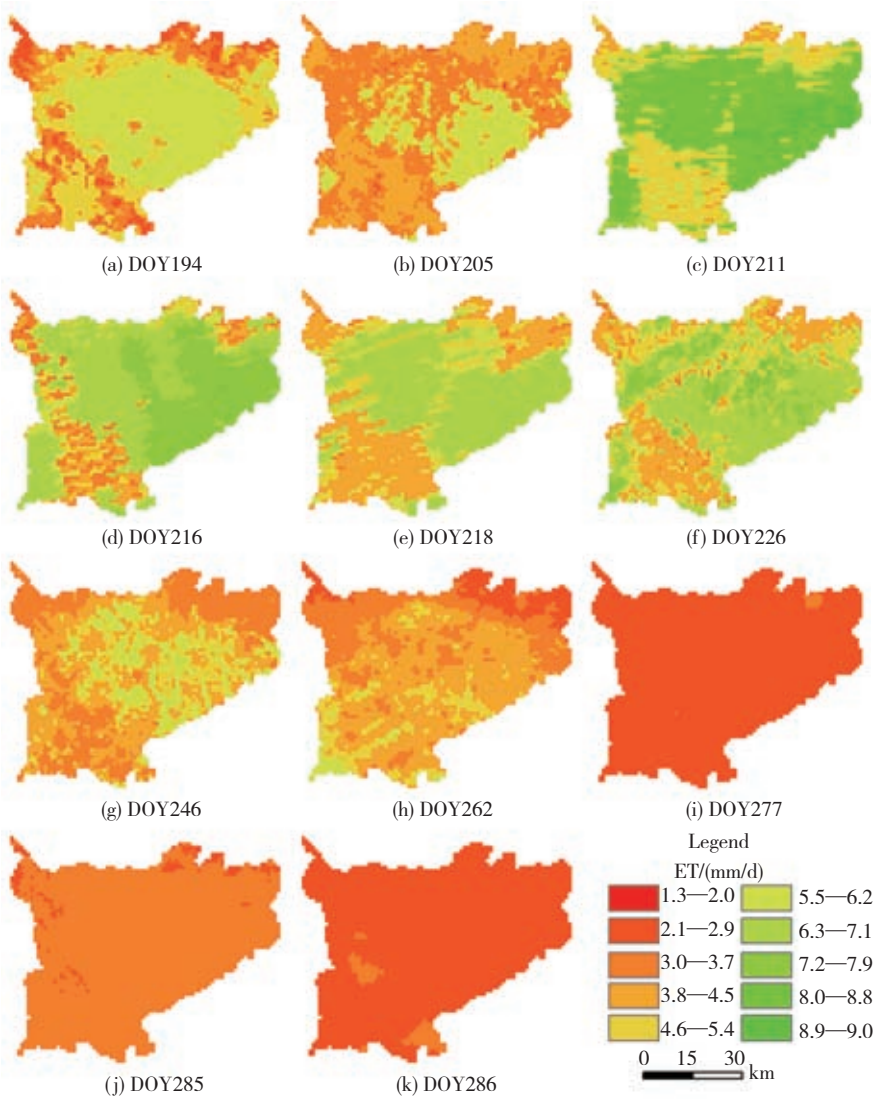

图2 太仆寺旗2008年生长季日蒸散发反演结果(1 km空间分辨率)

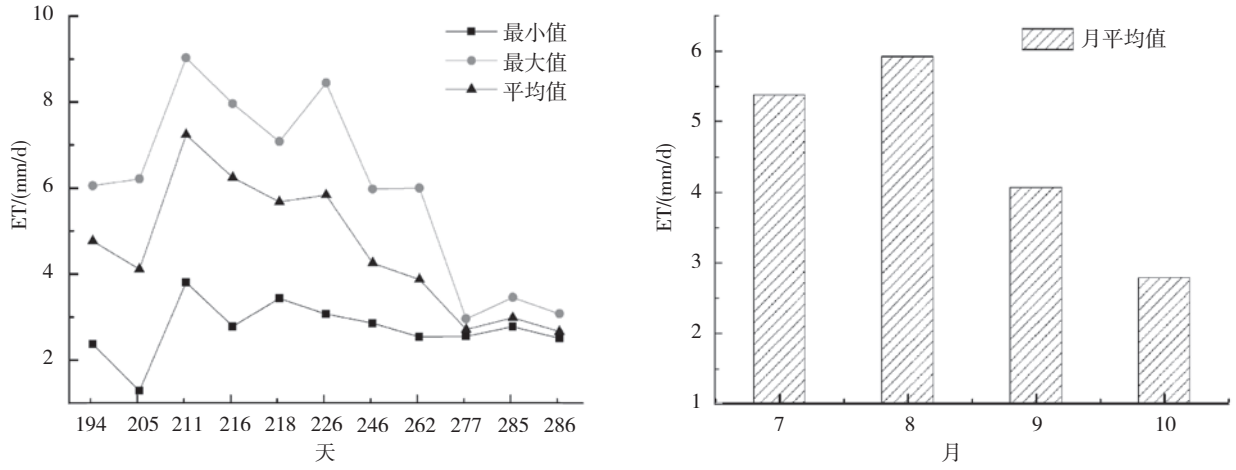

(a) 日值(最大、最小、平均值)变化趋势 (b) 月平均值变化趋势

图3 太仆寺旗蒸散发反演结果统计及其变化趋势

整体而言，本文模型反演的蒸散发量与观测值之间的最小绝对误差仅为0.11 mm/d，但最大绝对误差为2.78 mm/d，平均绝对误差为0.72 mm/d。就各波文比系统而言，2号系统处的反演精度较3号系统的略高，前者的平均绝对误差为0.64 mm/d，后者的为0.80 mm/d，其中：2号系统处的最大、最小绝对误差分别为0.11 mm/d、2.78 mm/d；3号系统处的最大、最小绝对误差分别为0.11 mm/d、1.64 mm/d。

在11天的21次对比验证中，模型反演结果对波文比系统观测结果的平均相对误差为20.76%，逐日相对误差小于0.1的占47.6%，介于0.1—0.2之间的占19.1%，介于0.2—0.3的占9.5%(表3)。就2号波文比系统而言，在10次对比验证中，逐日相对误差小于0.1的占60%，介于0.1—0.2之间的占20%，介于0.2—0.3的占10%。就3号波文比系统而言，在11次对比验证中，逐日相对误差小于0.1的占36.4%，介于0.1—0.2之间的占18.2%，介于0.2—0.3的占9.1%。

表2 三温模型反演的日蒸散发量与观测值对比结果

DOY	2号波文比系统				3号波文比系统			
	ET_β /mm	ET_M /mm	绝对误差 /mm	相对误差 /%	ET_β /mm	ET_M /mm	绝对误差 /mm	相对误差 /%
194	5.96	3.18	2.78	46.64	3.15	3.31	0.16	5.08
205	3.60	4.19	0.59	16.39	2.50	3.84	1.34	53.60
211	5.44	5.20	0.24	4.41	4.62	4.48	0.14	3.03
216	5.45	6.68	1.23	22.57	5.11	5.97	0.86	16.83
218	4.66	4.88	0.22	4.72	4.40	5.03	0.63	14.32
226	4.59	4.96	0.37	8.06	3.97	4.34	0.37	9.32
246	3.09	3.27	0.18	5.83	3.14	3.25	0.11	3.50
262	2.60	2.83	0.23	8.85	2.15	2.76	0.61	28.37
277	2.71	2.82	0.11	4.06	1.18	2.75	1.57	133.05
285	—	2.94	—	—	1.25	2.89	1.64	131.20
286	2.18	2.60	0.42	19.27	1.23	2.58	1.35	109.76
平均	4.03		0.64	15.81	2.97		0.80	26.80
平均绝对误差			0.72 mm		平均相对误差			20.76 %

注：ET_β为波文比系统观测值、ET_M为本文模型反演值—数据异常，不参与验证。

绝对误差=$|ET_\beta - ET_M|$　　相对误差=$|ET_\beta - ET_M|/ET_\beta$

平均绝对误差=$\sum(|ET_\beta - ET_M|)/n$

平均相对误差=$(100/\overline{ET_\beta})\sum(|ET_\beta - ET_M|)/n$

表3 相对误差等级比例统计

相对误差	单独统计/%		合并统计/%
	波文比系统2	波文比系统3	
<0.1	60.0	36.4	47.6
<0.2	20.0	18.2	19.1
<0.3	10.0	9.1	9.5
≥0.3	10.0	36.3	23.8

4.3 验证结果评价

根据波文比系统原始观测数据合理性分析评价验证结果。

(1)相对误差小于30%

相对误差小于30%的结果共16个，限于篇幅，仅选择DOY218的3号波文比系统作为代表分析，因其反演的相对误差为14.32%，最接近评价范围的中间值(15%)。图4(a)为对应的原始逐时观测数据，观测的净辐射、土壤热通量连续性好，无明显跳动(仅净辐射在15时左右有短暂波动)，波文比方法计算的潜热通量科学合理，表明以此验证本文模型反演结果是可信的。

(2)相对误差大于30%

对2号波文比系统，相对误差大于30%的有DOY194，在其对应的原始逐时观测数据中(图4(b))，虽然观测的净辐射与土壤热通量正常，但波文比法计算的大部分潜热通量大于净辐射(6—14时)，其余略小于净辐射(14时至日落)，由此计算的蒸散发结果异常。

对3号波文比系统，相对误差大于30%的有4天：DOY205、DOY277、DOY285、DOY286。

DOY205对应的原始逐时观测数据以12时为分界线，之前的净辐射、土壤热通量观测数据正常，之后的数据剧烈变化(图4(c))，考虑到该区域当日无降水记录，观测结果属于异常，由此计算的蒸散发结果异常。

DOY277、DOY285、DOY 286原始逐时观测数据的大小与变化规律相似，选择3天中相对误差处于中间的DOY285为代表分析。DOY285对应的原始逐时观测数据如图4(d)所示，净辐射、土壤热通量观测数据未见异常，波文比值亦正常(日平均为1.8)，计算的潜热通量(蒸散发)合理。

综上所述，在21次对比验证中，除2号波文比系统在DOY194与3号系统在DOY205的观测结果可能异常外，其他19次验证结果可靠。在观测点开展的地面水分收支实验(利用小蒸渗仪、TDR土壤水分仪等)，也证明了波文比系统获得的蒸散发精度高(Qiu 等，2011)。若只考虑这19次对比验证，基于遥感的三温模型反演的蒸散发量与观测值之间的最小、最大绝对误差分别为0.11 mm/d、1.64 mm/d，平均值绝对误差为0.58 mm/d。图5显示19次日蒸散发量验证散点图，

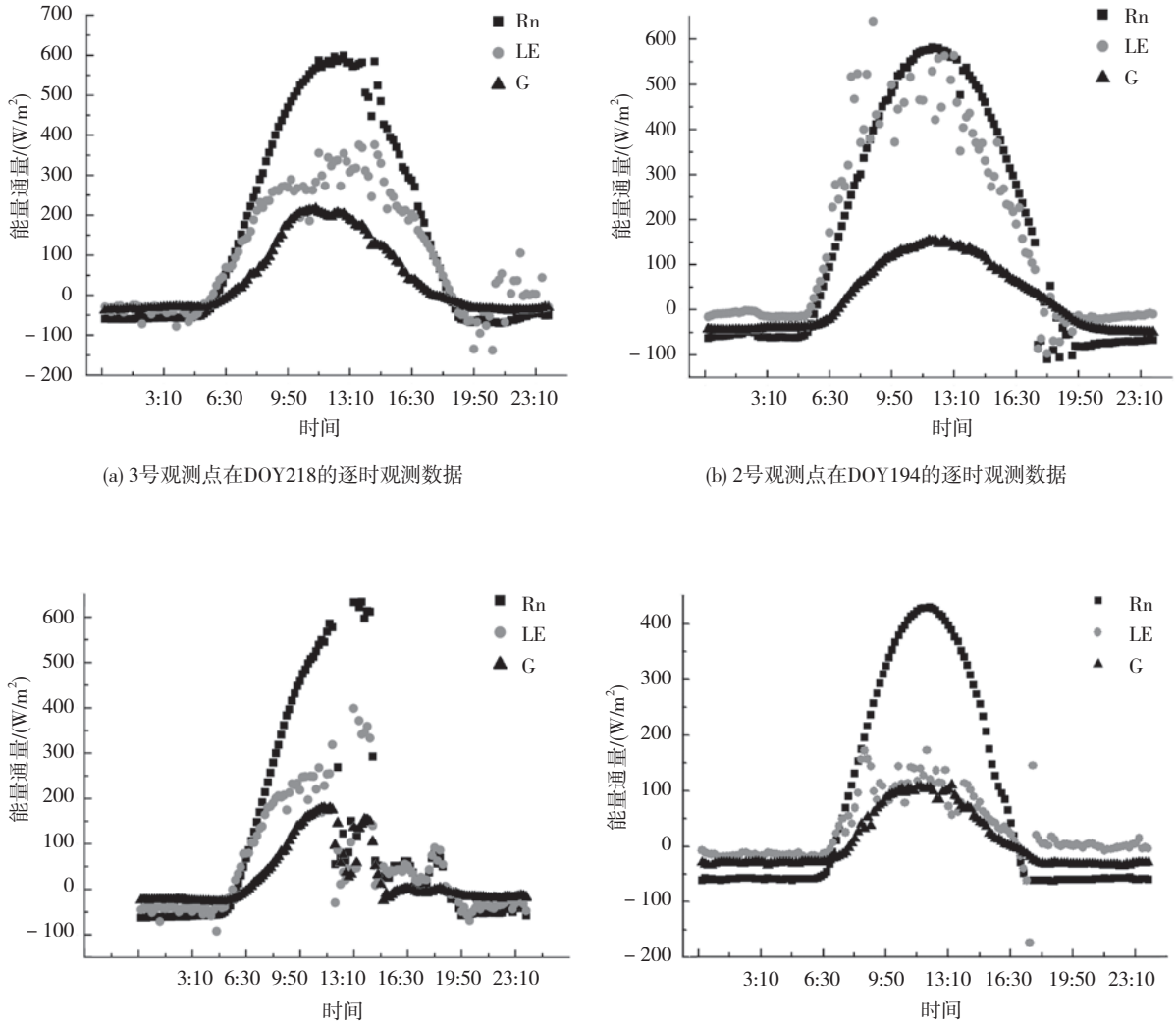

(a) 3号观测点在DOY218的逐时观测数据

(b) 2号观测点在DOY194的逐时观测数据

(c) 3号观测点在DOY205的逐时观测数据

(d) 3号观测点在DOY285的逐时观测数据

图4 逐时通量观测数据

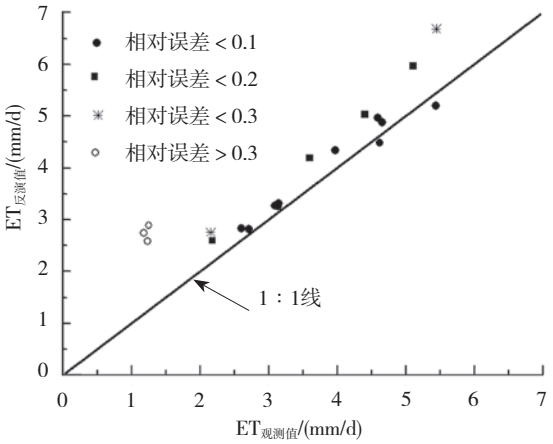

图5 日蒸散发量验证结果

大部分散点沿1：1线分布，本文模型反演结果对波文比系统观测结果的平均相对误差为17.10%。

鉴于MODIS L1B遥感影像的空间分辨率较粗，模型反演的参数不能有效反映下垫面的细微差别，如2、3号波文比观测系统相距仅有4.5 km、下垫面均为退耕草地(见图1)，但10月份两套系统观测的同日蒸散发出现明显差异，而模型反演的对应结果却无明显差异(表2)。以及波文比系统观测数据代表的范围小于1 km^2(Rana和Katerji，2000；Baldocchi，2003)，用其检验1 km尺度下3×3像元均值，存在一定的不确定性。此外，波文比观测系统的能量闭合程度对验证结果有影响。研究表明能量闭合率越接近1，蒸散发反演结果接近观测值的概率越大、反演结果越好(吴炳方 等，2008)。本文实验中无显热通量观测，不能研究波文比系统的能量闭合程度，根据岳平等人(2010)利用国家气象站的通量观测资料分析结果，内蒙古锡林郭勒草原在生长期(5—9月)的日平均能量不闭合程度为10%。本文研究区位于锡林郭勒草原的西南部，

近似假设模型验证期间的能量闭合率为90%。基于以上分析，本文虽然受到不确定性的影响，但结果是可靠的。

5 结 论

在内蒙古太仆寺旗的农田－草地生态系统国家野外站开展研究，以2008年植被生长季期间(7月—10月)的两套波文比系统观测数据检验三温模型在1 km空间尺度反演蒸散发的精度，得出以下结论：

(1) 经分析，本文选用无云MODIS L1B影像同期的22次观测结果中，两套波文比系统观测设备受局地气候等不确定性因素影响，导致观测的净辐射、土壤热通量或波文比值异常，计算的蒸散发量出现3次异常结果，但其他19次观测数据科学可信，观测结果正常；

(2) 基于三温模型与MODIS L1B影像反演的蒸散发量，在整个生长季的平均值、最大、最小值分别为4.58 mm/d、9.03 mm/d、1.28 mm/d；

(3) 模型精度评价结果表明：19次对比验证中，基于遥感的三温模型反演的蒸散发量与波文比系统观测结果之间的最小、最大绝对误差分别为0.11 mm/d、1.64 mm/d，平均绝对误差为0.58 mm/d；蒸散发反演结果对波文比系统观测结果的平均相对误差为17.10%。

志 谢 此次野外观测得到北京师范大学王佩、谢芳、冯右骏同学的帮助，在此表示衷心的感谢！

参考文献（References）

Aboukhaled A, Alfaro A and Smith M. 1982. FAO Irrigation and Drainage Paper No. 39, Lysimeters. Rome: FAO

Allen R G, Pereira L S, Raes D and Smith M. 1998. FAO Irrigation and drainage paper No. 56, Crop evapotranspiration-Guidelines for computing crop water requirements. Rome: FAO

Allen R G, Tasumi M, Morse A, Trezza R, Wright J L, Bastiaanssen W, Kramber W, Lorite I and Robison C W. 2007. Satellite-based energy balance for mapping evapotranspiration with internalized calibration (METRIC)-applications. Journal of Irrigation and Drainage Engineering, 133(4): 395–406 [DOI: 10.1061/(ASCE)0733-9437(2007)133:4(395)]

Andreas E L and Cash B A. 1996. A new formulation for the Bowen ratio over saturated surfaces. Journal of Applied Meteorology, 35(8): 1279–1289 [DOI: 10.1175/1520-0450-(1996)035<1279:ANFFTB>2.0.CO;2]

Baldocchi D D. 2003. Assessing the eddy covariance technique for evaluating carbon dioxide exchange rates of ecosystems: past, present and future. Global Change Biology, 9(4): 479–492 [DOI: 10.1046/j.1365–2486.2003.00629.x]

Bastiaanssen W G M. 2000. SEBAL-based sensible and latent heat fluxes in the irrigated Gediz Basin, Turkey. Journal of Hydrology, 229(1/2): 87–100 [DOI: 10.1016/S0022-1694(99)00202-4]

Bastiaanssen W G M, Menenti M, Feddes R A and Holtslag A A M. 1998. A remote sensing surface energy balance algorithm for land (SEBAL). 1. Formulation. Journal of Hydrology, 212–213: 198–212 [DOI: 10.1016/S0022-1694(98)00253-4]

Bowen I S. 1926. The ratio of heat losses by conduction and by evaporation from any water surface. Physical Review, 27(6): 779–798 [DOI: 10.1103/PhysRev.27.779]

Carlson T. 2007. An Overview of the “triangle method” for estimating surface evapotranspiration and soil moisture from satellite imagery. Sensors, 7(8): 1612–1629 [DOI: 10.3390/s7081612]

Elhaddad A, Garcia L A and Chávez J L. 2011. Using a surface energy balance model to calculate spatially distributed actual evapotranspiration. Journal of Irrigation and Drainage Engineering-ASCE, 137(1): 17–26 [DOI: 10.1061/(ASCE)IR.1943-4774.0000276]

Jia L, Su Z B, van den Hurk B, Menenti M, Moene A F, de Bruin H A R, Baselga Yrisarry J J, Ibanez M and Cuesta A. 2003. Estimation of sensible heat flux using the Surface Energy Balance System (SEBS) and ATSR measurements. Physics and Chemistry of the Earth, Parts A/B/C, 28(1/3): 75–88 [DOI: 10.1016/S1474-7065(03)00009-3]

Lhomme J P, Monteny B and Amadou M. 1994. Estimating sensible heat flux from radiometric temperature over sparse millet. Agricultural and Forest Meteorology, 68(1/2): 77–91 [DOI: 10.1016/0168-1923(94)90070-1]

刘绍民, 孙睿, 孙中平, 李小文, 刘昌明. 2004. 基于互补相关原理的区域蒸散量估算模型比较. 地理学报, 59(3): 331–340

Jackson R D, Hatfield J L, Reginato R J, Idso S B and Pinter P J Jr. 1983. Estimation of daily evapotranspiration from one time-of-day measurements. Agricultural Water Management, 7(1/3): 351–362 [DOI: 10.1016/0378-3774(83)90095-1]

Mo X G, Liu S X, Lin Z H and Zhao W M. 2004. Simulating temporal and spatial variation of evapotranspiration over the Lushi basin. Journal of Hydrology, 285(1/4): 125–142 [DOI: 10.1016/j.jhydrol.2003.08.013]

莫兴国, 林忠辉, 刘苏峡. 2000. 基于Penman-Monteith公式的双源模型的改进. 水利学报, 31(5): 6–11

Monteith J L. 1965. Evaporation and environment. Symposia of the Society for Experiment Biology, 19: 205–234

Norman J M, Kustas W P and Humes K S. 1995. Source approach for estimating soil and vegetation energy fluxes in observations of directional radiometric surface temperature. Agricultural and

Forest Meteorology, 77(3/4): 263–293 [DOI: 10.1016/0168-1923(95)02265-Y]

潘竟虎, 刘春雨. 2010. 基于TSEB平行模型的黄土丘陵沟壑区蒸散发遥感估算. 遥感技术与应用, 25(2): 183–188

Pauwels V R N and Samson R. 2006. Comparison of different methods to measure and model actual evapotranspiration rates for a wet sloping grassland. Agricultural Water Management, 82(1/2): 1–24 [DOI: 10.1016/j.agwat.2005.06.001]

Qiu G Y, Miyamoto K, Sase S, Gao Y, Shi P J and Yano T. 2002. Comparison of the three-temperature Model and conventional models for estimating transpiration. JARQ-Japan Agricultural Research Quarterly, 36(2): 73–82

Qiu G Y, Momii K and Yano T. 1996. Estimation of plant transpiration by imitation leaf temperature. I. Theoretical consideration and field verification. Transactions of the Japanese society of irrigation, Drainage and Reclamation Engineering, 183: 47–56

Qiu G Y, Shi P J and Wang L M. 2006. Theoretical analysis of a remotely measurable soil evaporation transfer coefficient. Remote Sensing of Environment, 101(3): 390–398 [DOI: 10.1016/j.rse.2006.01.007]

Qiu G Y, Xie F, Feng Y C and Tian F. 2011. Experimental studies on the effects of the “Conversion of Cropland to Grassland Program” on the water budget and evapotranspiration in a semi-arid steppe in Inner Mongolia, China. Journal of Hydrology, 411(1/2): 120–129 [DOI: 10.1016/j.jhydrol.2011.09.040]

Qiu G Y, Yano T and Momii K. 1998. An improved methodology to measure evaporation from bare soil based on comparison of surface temperature with a dry soil surface. Journal of Hydrology, 210(1/4): 93–105 [DOI: 10.1016/S0022-1694(98)00174-7]

Qiu G Y and Zhao M. 2010. Remotely monitoring evaporation rate and soil water status using thermal imaging and “three-temperatures model (3T Model)” under field-scale conditions. Journal of Environmental Monitoring, 12(3): 716–723 [DOI: 10.1039/B919887C]

Rana G and Katerji N. 2000. Measurement and estimation of actual evapotranspiration in the field under Mediterranean climate: a review. European Journal of Agronomy, 13(2/3): 125–153 [DOI: 10.1016/S1161-0301(00)00070-8]

Scott R L, Shuttleworth W J, Goodrich D C and Maddock T III. 2000. The water use of two dominant vegetation communities in a semiarid riparian ecosystem. Agricultural and Forest Meteorology, 105(1/3): 241–256 [DOI: 10.1016/S0168-1923-(00)00181-7]

Shuttleworth W J and Wallance J S. 1985. Evaporation from sparse crops-an energy combination theory. Quarterly Journal of the Royal Meteorological Society, 111(469): 839–855 [DOI: 10.1002/qj.49711146910]

Sobrino J A, Kharraz J EL and Li Z L. 2003. Surface temperature and water vapour retrieval from MODIS data. International Journal of Remote Sensing, 24(24): 5161–5182 [DOI: 10.1080/0143116031000102502]

Sobrino J A and Raissouni N. 2000. Toward remote sensing methods for land cover dynamic monitoring: application to Morocco. International Journal of Remote Sensing, 21(2): 353–366 [DOI: 10.1080/014311600210876]

Su Z. 2002. The Surface Energy Balance System (SEBS) for estimation of turbulent heat fluxes. Hydrology and Earth System Sciences, 6(1): 85–100 [DOI: 10.5194/hess-6-85-2002]

Sun Z G, Wang Q X, Matsushita B, Fukushima T, Ouyang Z and Watanabe M. 2009. Development of a simple remote sensing EvapoTranspiration model (Sim-ReSET): algorithm and model test. Journal of Hydrology, 376(3/4): 476–485 [DOI: 10.1016/j.jhydrol.2009.07.054]

Swinbank W C. 1951. The measurement of vertical transfer of heat and water vapor by eddies in the lower atmosphere. Journal of Meteorology, 8(3): 135–145 [DOI: 10.1175/1520-0469-(1951)008<0135:TMOVTO>2.0.CO;2]

田静, 苏红波, 孙晓敏, 陈少辉. 2009. 遥感反演土壤蒸发/植被蒸腾二层模型在华北地区的应用. 地理研究, 28(5): 1297–1306

Trenberth K E, Fasullo J T and Kiehl J. 2009. Earth’s global energy budget. Bulletin of the American Meteorological Society, 90(3): 311–323 [DOI: 10.1175/2008BAMS2634.1]

王庆改, 康跃虎, 刘海军, 刘士平. 2005. 喷灌对冠层水汽交换的影响. 农业工程学报, 21(1): 46–51

吴炳方, 熊隽, 闫娜娜, 杨雷东, 杜鑫. 2008. 基于遥感的区域蒸散量监测方法——ETWatch. 水科学进展, 19(5): 671–678

辛晓洲, 田国良, 柳钦火. 2003. 地表蒸散定量遥感的研究进展. 遥感学报, 7(3): 233–239

Xiong Y J and Qiu G Y. 2011. Estimation of evapotranspiration using remotely sensed land surface temperature and the revised three-temperature model. International Journal of Remote Sensing, 32(20): 5853–5874 [DOI: 10.1080/01431161.2010.507791]

徐新良, 刘纪远, 庄大方. 2004. GIS环境下1999－2000年中国东北参考作物蒸散量时空变化特征分析. 农业工程学报, 20(2): 10–14

岳平, 张强, 邓振镛, 杨金虎, 孙旭映. 2010. 草原生长期地表辐射和能量通量月平均日变化特征. 冰川冻土, 32(5): 941–947

张仁华, 孙晓敏, 王伟民, 许金萍, 朱治林, 田静. 2004. 一种可操作的区域尺度地表通量定量遥感二层模型的物理基础. 中国科学D辑, 34(S2): 200–216

赵长森, 夏军, 李召良, 刘玉, 唐伯惠, 唐荣林, 严子奇, 欧阳晓莹. 2008. 基于高时间分辨率静止卫星数据的区域耗水时空格局研究——以春旱季节淮河流域蚌埠以上农业区为例. 自然资源学报, 23(6): 1055–1067